

NANOSTRUCTURES

PACS numbers: 79.60.Dp; 79.60.Jv
DOI: 10.1070/QE2015v045n01ABEH015564

Bulk photoemission from metal films and nanoparticles

R.Sh. Ikhsanov, V.E. Babicheva, I.E. Protsenko, A.V. Uskov, M.E. Guzhva

Abstract. **Internal emission of photoelectrons from metal films and nanoparticles (nanowires and nanospheres) into a semiconductor matrix is studied theoretically by taking into account the jump of the effective electron mass at the metal–semiconductor interface and the cooling effect of hot electrons due to electron–electron collisions in the metal. The internal quantum efficiency of photoemission for the film and nanoparticles of two types (nanospheres and nanowires) is calculated. It is shown that the reduction of the effective mass of the electron during its transition from metal to semiconductor may lead to a significant (orders of magnitude and higher) decrease in the internal quantum efficiency of bulk photoemission.**

Keywords: *bulk photoemission, plasmonic nanoantennas, internal quantum efficiency, effective mass of the electron, Schottky barrier.*

1. Introduction

Recently, photodetectors based on resonant photoemission of electrons from plasmonic nanoantennas [1, 2] and metal films [3] have been proposed and experimentally demonstrated, which has resulted in exploring the possibility of using resonant photoemission in photovoltaics [4, 5]. In nanoantennas, i.e., nanometre-sized metal particles, resonant photoemission occurs upon excitation of localised oscillations of the electron density (localised surface plasmon resonance – LSPR) under the action of an external electromagnetic field of a certain frequency. The LSPR appearance leads to a significant increase in the electromagnetic field strength inside and around nanoantennas and, as a consequence, to an increase in the absorption of the electromagnetic field energy by the electrons of the metal. Accordingly, if the energy of the absorbed field quantum is sufficient for the electron of the metal (hot electron) that has absorbed this quantum to overcome the potential barrier at the matrix–nanoantenna interface, then the LSPR excitation is accompanied by a resonant increase in photoemission.

In addition to the plasmon resonance, an increase in the efficiency of photoemission from nanoantennas stems from their small size, i.e., in the case when the mean free path of the photoelectron is comparable with at least one of the nanoantenna dimensions, the hot electron has a higher (than in the case of photoemission from macrobodies) probability of reaching the nanoantenna boundary and go beyond it [3]. In this case, it is important to consider the cooling of hot electrons in electron–electron and electron–phonon collisions [5]. To account for the cooling of hot electrons, use is made of one of the most suitable techniques, i.e., the Monte Carlo method (see, e.g., [6]), which is however very cumbersome. In this connection, several approximate methods were developed (see papers [3, 5, 7, 8] and references therein). Below we use the model of the cooling of hot electrons, proposed in [7], to obtain a number of analytical results.

In metal films and nanoparticles, surface photoeffect can be quite pronounced [2, 8, 9], which is manifested in the fact that an electron absorbs a photon in a collision with the metal–semiconductor interface. In addition, there is also a bulk photoeffect – the process during which a photon is absorbed in the bulk of a nanoparticle, i.e., in a collision of a free electron of the metal with a phonon or a defect in the crystal lattice of the metal. Note that the detailed description of the absorption of a photon by an electron in collisions is not required for our purposes. Similarly to other works (see, e.g., [3, 5, 7]), we confine our consideration to the bulk photoeffect solely.

One of the main characteristics of photoemission is its internal quantum efficiency (IQE), i.e., the probability of passing the interface by a hot photoelectron. The problem of finding this probability is divided into two: calculation of the Schottky barrier shape at the metal–semiconductor matrix interface and calculation of the probability of overcoming of this barrier by a photoelectron. A detailed calculation of this barrier was performed in a number of studies [10, 11], but to compare the photoemission IQE from different nanoparticles, we use a simple approximation for its shape – a rectangular potential step with a height equal to the work function from metal into semiconductor. By excluding the image force, the work function is calculated as the difference between the work function from this metal into vacuum and the electron affinity of a semiconductor matrix.

For a barrier (in the form of a step) it is easy to find the exact quantum-mechanical expression for the probability that an electron will pass through the barrier, the jump of the

R.Sh. Ikhsanov Research Institute of Scientific Instruments of 'Rosatom' State Atomic Energy Corporation, promzona Turaevo, Bld. 8, 140080 Lytkarino, Moscow region, Russia; e-mail: ihsanov_renat@mail.ru;
V.E. Babicheva ITMO University, Kronverkskiy prosp. 49, 197101 St. Petersburg, Russia; Present address: Technical University of Denmark, Oersteds Plads, 343, Kgs. Lyngby, 2800, Denmark;
I.E. Protsenko, A.V. Uskov P.N. Lebedev Physics Institute, Russian Academy of Sciences, Leninsky prosp. 53, 119991 Moscow, Russia; Advanced Energy Technologies Ltd., ul. Novaya 100, 143025 Skolkovo, Russia, Moscow region;
M.E. Guzhva ITMO University, Kronverkskiy prosp. 49, 197101 St. Petersburg, Russia; Saint-Petersburg State Polytechnic University, ul. Politekhnicheskaya 29, 195251 St. Petersburg, Russia

Received 26 May 2014; revision received 4 August 2014
Kvantovaya Elektronika **45** (1) 50–58 (2015)
Translated by I.A. Ulitkin

effective electron mass at the interface being taken into account. As we will show below, the account for this jump is extremely important because it can significantly affect the effective barrier height and consequently the quantum yield of photoemission. Note that the effective masses of an electron in a metal nanoparticle and in a surrounding semiconductor may vary by more than an order of magnitude. For example, $m/m^* \approx 4$ for Au/Si and about 15 for Au/GaAs [12], where m and m^* are the effective masses of an electron in the metal and the semiconductor matrix, respectively. The need to take account of the effective mass jump in the calculation of the transmission coefficient of the potential barrier in the problem of photoemission has been noted previously [13, 14]. In this paper, we investigate in detail, in particular, the effect of this difference in the masses on photoemission from metal films and nanoparticles that are of interest for photodetectors and solar cells.

In Section 2 we present the methods for calculating the IQE of metal films and nanoparticles for the cases of both homogeneous and inhomogeneous electric field distributions in the metal within the framework of a three-step photoemission model with the account for inelastic scattering of hot electrons by 'cold' electrons of the metal. In Section 3 we describe the used models of the transmission coefficient of the potential barrier at the metal–semiconductor interface. In Section 4 we present formulas for the IQE of a flat film and nanoparticles of two simple shapes: spheres and wires of circular cross section. In Section 5 we discuss the spectral dependence of the IQE near the long-wavelength interface for a flat film, nanosphere and nanowire; namely, we compare the IQE for two cases: the exact quantum-mechanical solution for a rectangular potential step and approximation of the transmission coefficient by the Heaviside function. The obtained results and possible directions of further research on bulk photoemission from metal films and nanoparticles are discussed in Conclusions.

2. IQE of photoemission from metal films and nanoparticles

The general scheme of the phenomenon in question is shown in Fig. 1. A plane light wave of the form $\mathrm{Re}[\boldsymbol{E}_0\exp(-i\omega t)]$propagates in a semiconductor matrix with embedded metal nanoparticles (for brevity we speak, as a rule, of nanoparticles, bearing films in mind). Field $\boldsymbol{E}_i(\boldsymbol{r})$ inside a nanoparticle in the general case can be expressed as

$$\boldsymbol{E}_i(\boldsymbol{r}) = \hat{F}(\boldsymbol{r})\boldsymbol{E}_0, \tag{1}$$

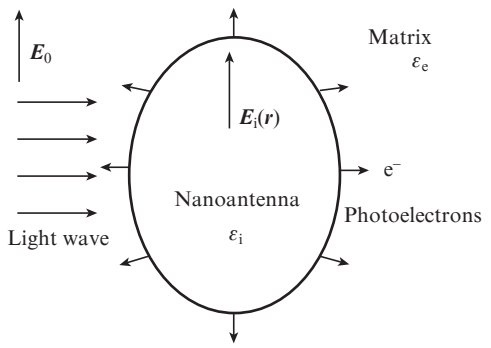

Figure 1. Metal nanoparticle in a semiconductor matrix.

where $\hat{F}(\boldsymbol{r})$ is the operator (matrix), which depends on the shape and size of the nanoparticle, field polarisation $\boldsymbol{E}_0$ with respect to the nanoparticle and dielectric constants $\varepsilon_i(\omega)$ and ε_e of the nanoparticle and matrix materials, respectively.

For the nanoparticles' shapes and the film under study, it is convenient to introduce the characteristic size L_n: for a sphere and a cylinder it is the diameter and for a film it is the thickness. If the nanoparticle is ellipsoidal, then in the quasistatic approximation, i.e., when the characteristic size of the nanoparticle is much smaller than the wavelength of light in the matrix, the field inside the nanoparticle is homogeneous [15] and the operator $\hat{F}(\boldsymbol{r})$ is independent of the coordinate $\boldsymbol{r}$ inside the particle: $\hat{F}(\boldsymbol{r}) \equiv \hat{F}$. If the incident field $\boldsymbol{E}_0$ is polarised along one of the axes of the ellipsoid, the field $\boldsymbol{E}_i$ is parallel to $\boldsymbol{E}_0$, i.e., the operator $\hat{F}$ is actually a scalar: $\hat{F}(\boldsymbol{r}) \equiv F$.

Bulk photoemission involves three stages [16, 17]. In the first stage the metal electrons in collisions with phonons, lattice defects or impurity atoms absorb photons of the incident electromagnetic wave with energy $\hbar\omega$ and are excited to energies exceeding the Fermi energy, i.e., become hot (Fig. 2). In the second stage hot electrons move to the nanoparticle boundary, losing on the way their energy (being cooled) in electron–electron and electron–phonon collisions. In the third stage photoelectrons penetrate into the matrix through the nanoparticle boundary (for simplicity, as a matrix material we consider an n-type semiconductor) or are reflected from the boundary back into the metal.

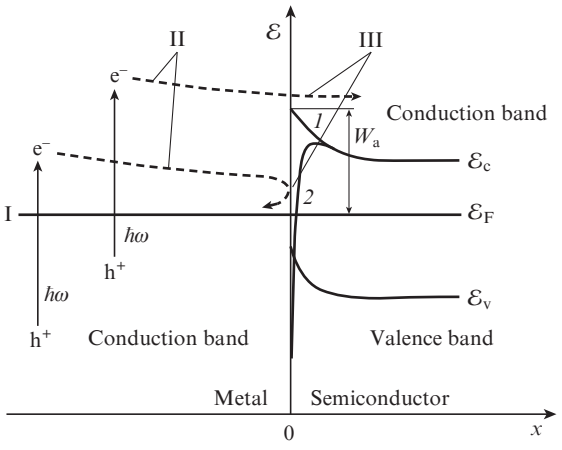

Figure 2. Three stages of bulk photoemission: I – excitation of the electrons of the metal (in collisions with phonons or lattice defects) from the occupied energy states in the conduction band into the unoccupied states above the Fermi level $\mathcal{E}_F$; II – electron transport in the metal; III – interaction of electrons with a Schottky barrier (overcoming of a barrier or reflection from it). Curve (*1*) shows the Schottky barrier without image forces, curve (*2*) – taking these forces into account; W_a is the work function from the metal into the semiconductor; and $\mathcal{E}_v$ and $\mathcal{E}_c$ is the top of the valence band and the bottom of the conduction band of the semiconductor, respectively.

Obviously, the specific rate of photoemission, $r_{em}(\boldsymbol{r})$ (in s^{-1} m^{-3}), which describes photoemission from nanoparticles upon excitation of hot electrons at point $\boldsymbol{r}$ on the nanoparticle, is proportional to the specific rate of absorption of photons in the metal nanoparticle, $r_{abs}(\boldsymbol{r})$ (in s^{-1} m^{-3}):

$$r_{em}(\boldsymbol{r}) = \eta_i^{local}(\boldsymbol{r})\, r_{abs}(\boldsymbol{r}). \tag{2}$$

The proportionality factor $\eta_i^{local}(\boldsymbol{r})$ is, by definition, the local IQE of photoemission – the probability that a photoelectron, which has absorbed a photon at point $\boldsymbol{r}$, experiences photoemission, i.e., will reach the nanoparticle boundary and go beyond it. The specific rate of photon absorption, r_{abs}, [15] can be expressed in terms of the imaginary part ε_i'' of the dielectric constant of the metal, ε_i ($\varepsilon_i = \varepsilon_i' + i\varepsilon_i''$), and the field strength in the nanoparticle:

$$r_{abs}(\boldsymbol{r}) = \frac{1}{2}\frac{\varepsilon_0\varepsilon_i''}{\hbar}|\boldsymbol{E}_i(\boldsymbol{r})|^2 = \frac{1}{2}\frac{\varepsilon_0\varepsilon_i''}{\hbar}|\hat{F}(\boldsymbol{r})\boldsymbol{E}_0|^2. \quad (3)$$

We can write a relation, similar to (2), for the entire nanoparticle and thus determine its IQE, η_i:

$$R_{em} = \eta_i R_{abs}, \quad (4)$$

where R_{abs} and R_{em} are the rates of photon absorption and photoelectron emission from the nanoparticle, respectively (in s^{-1});

$$R_{abs} = \int_{V_n} r_{abs}(\boldsymbol{r})\,d^3r, \quad R_{em} = \int_{V_n} r_{em}(\boldsymbol{r})\,d^3r; \quad (5)$$

$$\eta_i = \int_{V_n} \eta_i^{local}(\boldsymbol{r})\,|\hat{F}(\boldsymbol{r})\boldsymbol{E}_0|^2 d^3r \Big/ \int_{V_n} |\hat{F}(\boldsymbol{r})\boldsymbol{E}_0|^2 d^3r; \quad (6)$$

and V_n is the nanoparticle volume. Obviously, the IQE in formula (6) [when $\hat{F}$ is the linear operator (the field strength is not too large, and nonlinear effects can be neglected)] does not depend on the modulus of the vector $\boldsymbol{E}_0$. In the case of a homogeneous field in the nanoparticle, when the scalar $\hat{F}$ is independent of $\boldsymbol{r}$, it follows from (6) that

$$\eta_i = \frac{1}{V_n}\int_{V_n} \eta_i^{local}(\boldsymbol{r})\,d^3r, \quad (7)$$

i.e. η_i in this case is the local IQE averaged over the nanoparticle volume.

The local IQE entering expressions (6) and (7) can be found as follows. Specific absorption $r_{abs}(\boldsymbol{r})$ can be written as

$$r_{abs}(\boldsymbol{r}) = |\boldsymbol{E}_i(\boldsymbol{r})|^2 \int B(\boldsymbol{k}',\boldsymbol{k})[f_e(\mathcal{E}(k')) - f_e(\mathcal{E}(k))] \times \delta(\mathcal{E}(\boldsymbol{k}') - \mathcal{E}(\boldsymbol{k}) + \hbar\omega)\,d^3k\,d^3k', \quad (8)$$

where $f_e(\mathcal{E})$ is the Fermi function of the electron distribution in energy $\mathcal{E}$; integration over $d^3k = k^2 dk d\Omega_k$ includes integration over moduli k of the wave vectors $\boldsymbol{k}$ (dk) and their directions ($d\Omega_k$); similarly – integration over $d^3k' = k'^2 dk' d\Omega_k$; the function $B(\boldsymbol{k}',\boldsymbol{k})$) describes the induced transition from a state with the wave vector $\boldsymbol{k}'$ to a state with the wave vector $\boldsymbol{k}$ with the absorption of a photon [correspondingly, $B(\boldsymbol{k},\boldsymbol{k}')$ describes the transition from a state with the wave vector $\boldsymbol{k}$ to a state with the wave vector $\boldsymbol{k}'$ with the emission of a photon]; and $B(\boldsymbol{k}',\boldsymbol{k}) = B(\boldsymbol{k},\boldsymbol{k}')$. In formula (8) the integral over d^3k' denotes summation over all the initial states of the electrons, and the integral over d^3k – averaging over all possible final states for each initial state.

We assume that the distribution density of the electron energy states in the metal corresponds to the isotropic parabolic dispersion law: $\mathcal{E} \propto k^2$. Performing in (8) the integration over d^3k' with account for the delta function $\delta(\mathcal{E}(\boldsymbol{k}') - \mathcal{E}(\boldsymbol{k}) + \hbar\omega)$ and the fact that $\mathcal{E}(k) = (\hbar k)^2/(2m)$, we obtain

$$r_{abs}(\boldsymbol{r}) = \int r_{exc}(\boldsymbol{r},\boldsymbol{k})\,d^3k, \quad (9)$$

where

$$r_{exc}(\boldsymbol{r},\boldsymbol{k}) = |\boldsymbol{E}_i(\boldsymbol{r})|^2 \times B'(k)[f_e(\mathcal{E}(k) - \hbar\omega) - f_e(\mathcal{E}(k))]\sqrt{\mathcal{E}(k) - \hbar\omega} \quad (10)$$

is the specific excitation rate in the phase space (in $s^{-1}\,m^{-3}\,m^3 = s^{-1}$). Additional constant factors arising from the integration in (8) are included in $B'(k)$. Then, we can introduce a specific photoemission rate $r_{em}(\boldsymbol{r})$, which is different from $r_{abs}(\boldsymbol{r})$ (9) by the factor $P_{em}(\boldsymbol{r},\boldsymbol{k})$ under the integral [$P_{em}(\boldsymbol{r},\boldsymbol{k})$ is the probability of emission of a photoelectron excited at point $\boldsymbol{r}$ with the wave vector $\boldsymbol{k}$]:

$$r_{em}(\boldsymbol{r}) = |\boldsymbol{E}_i(\boldsymbol{r})|^2 \int P_{em}(\boldsymbol{r},\boldsymbol{k})B'(k) \times [f_e(\mathcal{E}(k) - \hbar\omega) - f_e(\mathcal{E}(k))]\sqrt{\mathcal{E}(k) - \hbar\omega}\,d^3k. \quad (11)$$

Thus, according to (7)

$$\eta_i^{local}(\boldsymbol{r}) = \frac{\int P_{em}(\boldsymbol{r},\boldsymbol{k})B'(k)[f_e(\mathcal{E}(k) - \hbar\omega) - f_e(\mathcal{E}(k))]\sqrt{\mathcal{E}(k) - \hbar\omega}\,d^3k}{\int B'(k)[f_e(\mathcal{E}(k) - \hbar\omega) - f_e(\mathcal{E}(k))]\sqrt{\mathcal{E}(k) - \hbar\omega}\,d^3k}. \quad (12)$$

Expression (12) can be greatly simplified by assuming the product $B'(k)\sqrt{\mathcal{E}(k) - \hbar\omega}$ to be independent of k. This assumption dates back to the classical statistical theory of the Fowler photoelectric effect [18]. In this case, it is obvious that

$$\eta_i^{local}(\boldsymbol{r}) = \frac{\int P_{em}(\boldsymbol{r},\boldsymbol{k})[f_e(\mathcal{E}(k) - \hbar\omega) - f_e(\mathcal{E}(k))]d^3k}{\int [f_e(\mathcal{E}(k) - \hbar\omega) - f_e(\mathcal{E}(k))]\,d^3k}. \quad (13)$$

Note that if $B'(k)\sqrt{\mathcal{E}(k) - \hbar\omega}$ does not depend on k, the dependence of $r_{exc}(\boldsymbol{r},\boldsymbol{k})$ on k is determined only by the difference of the Fermi functions $f_e(\mathcal{E}(k) - \hbar\omega) - f_e(\mathcal{E}(k))$ [see Eqn (10)].

The influence of the thermal excitation of electrons on the spectral characteristics of the metal–semiconductor contact can be neglected at photon energies that are greater than the work function from the metal into the semiconductor, W_a, by $(2-3)k_BT$ (k_B is the Boltzmann constant, and T is the temperature) [19, 20]. By neglecting the thermal excitation of electrons located above the Fermi surface, $\mathcal{E}_F$ (i.e., assuming $T = 0$), it is easy to obtain that the difference $f_e(\mathcal{E}(k) - \hbar\omega) - f_e(\mathcal{E}(k))$ in the above formulas is equal to unity in the region $\mathcal{E}_F < \mathcal{E} < \mathcal{E}_F + \hbar\omega$ and to zero outside this region. Therefore, the specific rate of excitation in the phase space, $r_{exc}(\boldsymbol{r},\boldsymbol{k})$, differs from zero only in the layer

$$k_F < k < k_{\hbar\omega} \quad (13a)$$

of the phase space above the Fermi surface of the metal, where $\hbar k_F = \sqrt{2m\mathcal{E}_F}$ and $\hbar k_{\hbar\omega} = \sqrt{2m(\mathcal{E}_F + \hbar\omega)}$. At $T = 0$

the assumption that $B'(k)\sqrt{\mathcal{E}(k)-\hbar\omega}$ is independent of k means that the pump rate of hot electrons to the phase layer (13a) is uniform, i.e., does not depend on k:

$$r_{\text{exc}}(\boldsymbol{r},\boldsymbol{k}) = |\boldsymbol{E}_{\text{i}}(\boldsymbol{r})|^2\bar{B}, \tag{13b}$$

where $\bar{B} \equiv B'(k)\sqrt{\mathcal{E}(k)-\hbar\omega}$. Accordingly, expression (9) for the specific absorption can be rewritten as

$$r_{\text{abs}}(\boldsymbol{r}) = |\boldsymbol{E}_{\text{i}}(\boldsymbol{r})|^2\bar{B}V_k, \tag{13c}$$

where $V_k = 4\pi(k_{\hbar\omega}^3 - k_{\text{F}}^3)/3$ is the volume of the phase layer (13a). Note that by comparing relations (13c) and (3), we can express the coefficient $\bar{B}$ and hence the specific excitation rate $r_{\text{exc}}(\boldsymbol{r},\boldsymbol{k})$ through the imaginary part ε_{i}'' of the dielectric constant ε_{i} of the metal.

At $T = 0$ from (13) we obtain

$$\eta_{\text{i}}^{\text{local}}(\boldsymbol{r}) = \frac{1}{V_k}\int_{V_k} P_{\text{em}}(\boldsymbol{r},\boldsymbol{k})\,\mathrm{d}^3k. \tag{13d}$$

Thus, the local photoemission rate $r_{\text{em}}(\boldsymbol{r})$ can be computed using formulas (2), (3) and (13d), and thereafter the photoemission rate R_{em} and IQE of the nanoparticle can be calculated by formulas (5) and (7), respectively.

To account for the scattering of photoelectrons we use here a simple model considered in [7] (see also its description in [8]), which makes it possible, in some cases, to obtain analytical expressions for the IQE. It is assumed in this model that multiple reflections of the electrons from the boundary can be neglected; therefore, the probability $P_{\text{em}}(\boldsymbol{r},\boldsymbol{k})$ in (13d) is represented as

$$P_{\text{em}}(\boldsymbol{r},\boldsymbol{k}) = D(\mathcal{E}(k),\alpha(\boldsymbol{r},\boldsymbol{e}_k))\exp[-L(\boldsymbol{r},\boldsymbol{e}_k)/l_{\text{e}}], \tag{14}$$

where D is the coefficient of the photoelectron transmission through a barrier at the interface; α is the angle of incidence of photoelectrons at the interface; $\boldsymbol{e}_k = \boldsymbol{k}/|\boldsymbol{k}|$ is the unit vector, co-directional with the vector $\boldsymbol{k}$; L is the distance along a straight line from the point of generation of a photoelectron to the boundary; and l_{e} is the mean free path in electron–electron scattering. Here we assume that the photoelectron moves along a straight line from the point of its generation to the boundary. In addition, in the first electron–electron scattering event, the photoelectron loses approximately half its excess (relative to the Fermi level) energy [6]; therefore, it can be treated as the one that has not overcome the potential barrier at the interface. Thus, the likelihood that the photoelectron reaches the boundary is equal to the probability that the photoelectron will experience no electron–electron scattering events on its way to the boundary and, therefore, will not lose the energy, and this probability is taken into account by the factor $\exp(-L/l_{\text{e}})$. Note that the mean free path in electron–electron scattering is, generally speaking, a function of the electron excess energy above the Fermi level rather than a constant. The influence of this dependence on the quantum efficiency of photoemission was considered in [21, 22]. In this paper we consider a narrow range of photon energies near the long-wavelength boundary, and so this dependence is neglected. In addition, it is possible to take it into account only by numerical methods.

Electron–phonon scattering in model (14) is completely ignored, because scattering by phonons is almost elastic. Electron energy loss in a single event of collision with a phonon is ~3.10 eV, and the mean free path of electrons in electron–phonon collisions for gold and silver nanoparticles is ~50 nm [6]. For nanoparticles with characteristic dimensions less than 100 nm, this means a loss of no more than tenths of a percent of the initial electron energy on the way from the point of generation to the boundary, which in this case can be neglected.

3. Calculation of the transmission coefficient of the potential barrier at the nanoparticle–matrix interface

To calculate the transmission coefficient D [appearing in (14)] of the potential barrier at the nanoparticle–matrix interface, we assume that the photoelectron – a plane wave with the wave vector $\boldsymbol{k}_0$ – falls from medium 1 at the interface between media 1 (metal) and 2 (surrounding semiconductor matrix), which is subjected to the action of a potential in the form of a rectangular step of height W (Fig. 3). The interface between the media will also be assumed to be locally flat. This approximation is fulfilled when the de Broglie wavelength of the photoelectron is much smaller than the radius of curvature of the nanoparticle surface in place where the electron passes through the interface between the media. Despite the fact that, in general, reflection of hot electrons from the boundary is of mirror-diffuse nature [23], we use below the model of specular reflection, which is commonly used in the theory of the photoelectric effect [24] when it is assumed that the wave vector $\boldsymbol{k}_1$ of the reflected wave lies in the plane of incidence of the electron on the boundary and the angle of reflection equals the angle of incidence.

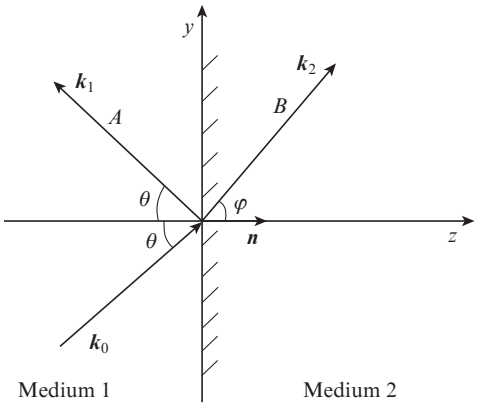

Figure 3. Schematic representation of the passage of the photoelectron through the interface between two media and its reflection from the interface.

Let us assume that the amplitude of the incident wave is equal to 1, that of the reflected wave – to A and that of the refracted wave – to B. In addition, we take into account that $k_0 = k_1$. Thus, the electron wave function can be written as

$$\begin{cases}\psi_1(\boldsymbol{r}) = \exp(\mathrm{i}\boldsymbol{k}_0\boldsymbol{r}) + A\exp(\mathrm{i}\boldsymbol{k}_1\boldsymbol{r}) \text{ in medium 1,}\\ \psi_2(\boldsymbol{r}) = B\exp(\mathrm{i}\boldsymbol{k}_2\boldsymbol{r}) \text{ in medium 2,}\end{cases} \tag{15}$$

where $k_i = \sqrt{2m_i(\mathcal{E}-U_i)}/\hbar$; $U_i = 0$ at $i = 1$ and $U_i = W$ at $i = 2$; $m_1 = m$, $m_2 = m^*$ (m and m^* are the effective masses of the electron in the metal and the matrix, respectively); and $\mathcal{E}$ is

the kinetic energy of the incident electrons ($\mathcal{E} > W$). Two boundary conditions (Bastard conditions [25]) are imposed on the wave function (15): the continuity of the wave function

$$\psi_1(\mathrm{O}) = \psi_2(\mathrm{O}) \tag{16}$$

and the continuity of the normal component of the probability flux density through the boundary, leading to the condition

$$\frac{1}{m}\boldsymbol{n}\nabla\psi_1\Big|_{\mathrm{O}} = \frac{1}{m^*}\boldsymbol{n}\nabla\psi_2\Big|_{\mathrm{O}}, \tag{17}$$

where O is an arbitrary point on the boundary, and $\boldsymbol{n}$ is unit vector of the normal to the boundary (Fig. 3). In addition, from the condition of specular reflection of the electron from the boundary follows the continuity of the tangential component of the wave vector of the electron:

$$k_0\sin\theta = k_2\sin\varphi, \tag{18}$$

where θ is the angle of incidence of the electron on the boundary. From equations (15)–(18) we obtain the unknown quantities:

$$A = \frac{1-\zeta}{1+\zeta}, \quad B = \frac{2}{1+\zeta}, \quad \zeta = r_m\frac{k_2}{k_0}\frac{\cos\varphi}{\cos\theta},$$
$$\varphi = \begin{cases} \arcsin\left(\dfrac{k_0}{k_2}\sin\theta\right), & \dfrac{k_0}{k_2}\sin\theta < 1, \\ \dfrac{\pi}{2}, & \dfrac{k_0}{k_2}\sin\theta \geqslant 1, \end{cases} \tag{19}$$

where $r_m = m/m^*$. Using (19), the transmission coefficient D can be determined as the ratio of the normal components of the probability flux density vector on both sides of the interface:

$$D = \mathrm{Re}\left(r_m\frac{k_{2z}}{k_{0z}}B^2\right) = \mathrm{Re}\left[\frac{4\zeta}{(1+\zeta)^2}\right]. \tag{20}$$

It is convenient to rewrite this formula in a form similar to the formula in the case of normal incidence of the electron on the rectangular potential step in the absence of a jump of its effective mass (see, e.g., [26]):

$$D_{\mathrm{q}} = \mathrm{Re}\left\{4\frac{[r_m(1-U_\rho/\mathcal{E}_z)]^{1/2}}{\{1+[r_m(1-U_\rho/\mathcal{E}_z)]^{1/2}\}^2}\right\}, \tag{21}$$

where

$$U_\rho = W + (r_m - 1)\mathcal{E}_\rho;\ \mathcal{E}_\rho = \mathcal{E}\sin^2\theta;$$
$$\mathcal{E}_z = \mathcal{E}\cos^2\theta;\ \mathcal{E} = \hbar^2k_0^2/(2m); \tag{22}$$

$\mathcal{E}_z$ is the electron kinetic energy associated with the normal component (to the interface) of its momentum; and similarly, $\mathcal{E}_\rho$ is the kinetic energy associated with the tangential component. Model dependence (21) is called the model of a rectangular potential step. In this case, the transmission coefficient depends on $\mathcal{E}_z$ and the effective barrier height U_ρ, which is dependent on the $\mathcal{E}_\rho$. In the case of $r_m > 1$ and oblique incidence of the electron onto the interface between the media, U_ρ is always greater than W by the value of the jump (positive) $\mathcal{E}_\rho$ during transition from medium 1 to medium 2. This leads to the fact that the maximum angle of incidence of the electron with fixed energy $\mathcal{E}$ onto the interface at which it still overcomes the potential barrier

$$\theta_{\max}(\mathcal{E}) = \arccos\left[\frac{1}{r_m}\left(\frac{W}{\mathcal{E}} + r_m - 1\right)\right]^{1/2}, \tag{23}$$

decreases monotonically with increasing r_m, i.e., the electron exit cone narrows down. Accordingly, the IQE of the nanoparticle decreases.

For the transmission coefficient, a simpler model is widely used in the literature (see, e.g., [17–19]) than the rectangular potential step model. For the transmission coefficient this model uses the Heaviside function:

$$D_{0-1}(\mathcal{E}_z) = \Theta(\mathcal{E}_z - U_\rho), \tag{24}$$

wheree $\mathcal{E}_z$ and U_ρ are defined by formulas (22). Model dependence (24) will be called the '0–1' model. In the case of $r_m = 1$ = 1 and arbitrary angle of incidence or arbitrary $r_m = 1$ and normal incidence, the '0–1' model describes the classical transmission coefficient. The value of this simple model is, *inter alia*, in that in many cases it allows one to obtain analytical results for the IQE of nanoparticles. Expressions (21) and (24) for the transmission coefficient are limiting and correspond to an extremely sharp (rectangular step) and extremely smooth [$W(x) = W$ for $x \in (-\infty, +\infty)$] change in the potential at the interface between the media. Therefore, it can be assumed that the IQE values calculated for any other potentials (at least those for which the tunnelling effects are insignificant) will lie between the values calculated for the two potentials: maximum IQE values correspond to the '0–1' model, and the minimum ones – to the rectangular potential step model.

4. IQE for films and nanoparticles

In this and following sections, the calculations are carried out under the assumption that the electric field is uniform in the nanoparticle. In this case, the IQE of the nanoparticle is calculated by formula (7), in which the local IQE has the form

$$\eta_{\mathrm{i}}^{\mathrm{local}}(\boldsymbol{r}) = \frac{1}{V_k}\int_{V_k} D(\mathcal{E}(k),\alpha(\boldsymbol{r},\boldsymbol{e}_k))\exp\left[-\frac{L(\boldsymbol{r},\boldsymbol{e}_k)}{l_{\mathrm{e}}}\right]\mathrm{d}^3k, \tag{25}$$

where $V_k = 4\pi(k_{\hbar\omega}^3 - k_{\mathrm{F}}^3)/3$. The integral in (25) can be conveniently written in spherical coordinates:

$$\eta_{\mathrm{i}}^{\mathrm{local}}(\boldsymbol{r}) = \frac{1}{V_k}\int_0^{2\pi}\mathrm{d}\varphi\int_0^{\pi}\mathrm{d}\theta\int_{k_{\mathrm{F}}}^{k_{\hbar\omega}}k^2\sin\theta$$
$$\times D(\mathcal{E}(k),\alpha(\boldsymbol{r},\theta,\varphi))\exp\left[-\frac{L(\boldsymbol{r},\theta,\varphi)}{l_{\mathrm{e}}}\right]\mathrm{d}k. \tag{26}$$

Using (26) we calculate the IQE for three simple objects: a flat film, a nanowire with a circular cross section and a nanosphere. As will be shown below, due to the presence of the symmetry axes, the IQE in these cases can be calculated analytically. In the general case, the corresponding integrals are evaluated numerically.

4.1. Flat film

First, we consider the case of a flat film (Fig. 4a). The auxiliary coordinate system $x'y'z'$, from the axes of which the

angles of the spherical coordinate system are measured (θ – от z' and φ – from x'), is oriented so that the z' axis is perpendicular to the film surface, and the other axes are oriented arbitrarily. Integrals (7) and (26) can be written as

$$\eta_{\rm i} = \int_0^1 \eta_{\rm i}^{\rm local}(\xi)\,{\rm d}\xi, \tag{27}$$

$$\eta_{\rm i}^{\rm local}(\xi) = \frac{3}{2}(k_{\hbar\omega}^3 - k_{\rm F}^3)^{-1} N_{\rm sd} \int_0^{\pi/2} {\rm d}\theta \int_{k_{\rm F}}^{k_{\hbar\omega}} I_{\rm f}(k,\xi,\theta)\,{\rm d}k, \tag{28}$$

where $N_{\rm sd} = 1,2$ is the number of sides of the film, through which the photoemission occurs; $\xi = x/L_{\rm f}$; x is the distance to the film surface; $L_{\rm f}$ is the film thickness;

$$I_{\rm f}(k,\xi,\theta) = k^2 \sin\theta \times D(\mathcal{E}(k),\alpha(\xi,\theta)) \exp\left[-\frac{L(\xi,\theta)}{l_{\rm e}}\right]; \text{ and}$$
$$\alpha(\xi,\theta) = \theta;\ L(\xi,\theta) = \xi L_{\rm f}/\cos\theta. \tag{29}$$

In the case of the '0–1' model at $r_m = 1$ and $l_{\rm e} = \infty$, calculating integral (27) we obtain

$$\eta_{\rm i} = \frac{N_{\rm sd}}{2}\frac{1}{(\delta^{3/2}-1)}\left(\frac{1}{2}\gamma^{-3/2} - \frac{3}{2}\gamma^{-1/2}\delta + \delta^{3/2}\right), \tag{30}$$

where $\delta = 1 + \hbar\omega/\mathcal{E}_{\rm F}$; $\gamma = \mathcal{E}_{\rm F}/W$; and $W = \mathcal{E}_{\rm F} + W_{\rm a}$.

4.2. Nanowire

Consider now the case of a nanowire with a circular cross section (Fig. 4b). The coordinate system $x'y'z'$ is oriented so that the z' axis is perpendicular to the side surface of the cylinder and the x' axis is parallel to the cylinder axis. Integrals (7) and (26) will be rewritten in the form

$$\eta_{\rm i} = 2\int_0^1 \eta_{\rm i}^{\rm local}(\xi)\xi\,{\rm d}\xi, \tag{31}$$

$$\eta_{\rm i}^{\rm local}(\xi) = \frac{3}{2\pi}(k_{\hbar\omega}^3 - k_{\rm F}^3)^{-1} \times \int_0^{\pi}{\rm d}\theta \int_0^{\pi}{\rm d}\phi \int_{k_{\rm F}}^{k_{\hbar\omega}} I_{\rm cyl}(k,\xi,\theta,\phi)\,{\rm d}k, \tag{32}$$

where $\xi = r/R$; r is the distance to the axis of the cylinder; R is the radius of the cylinder; and the function $I_{\rm cyl}(k,\xi,\theta,\phi)$ is written analogously to $I_{\rm f}(k,\xi,\theta)$ in formula (29) with the only exception that the functions α and L from the integration variables now have the form $\alpha(\xi,\theta,\varphi)$ and $L(\xi,\theta,\phi)$ and are determined by solving the problem of the intersection of the straight line, given in parametric form $\boldsymbol{r} = \boldsymbol{r}(s)$, with the cylinder surface. The corresponding system of equations (with respect to the variables s, y and z) has the form

$$\boldsymbol{r}(s) = \boldsymbol{r}_0 + \boldsymbol{e}_k s,$$
$$y^2 + z^2 = R^2, \tag{33}$$

where $\boldsymbol{r} = (x,y,z)$; $\boldsymbol{r}_0 = (0,0,\xi R)$; $\boldsymbol{e}_k = (\sin\theta\cos\varphi,\ \sin\theta\sin\varphi,\ \cos\theta)$; and the first equation is written only for the y- and z-components of the vectors. If s_0 is the solution to system (33), then $L = |\boldsymbol{e}_k s_0|$, and the angle α is determined as the angle of intersection of the vectors $\boldsymbol{e}_k$ and $\boldsymbol{n}_{\rm s} = (0,-y(s_0),-z(s_0))$.

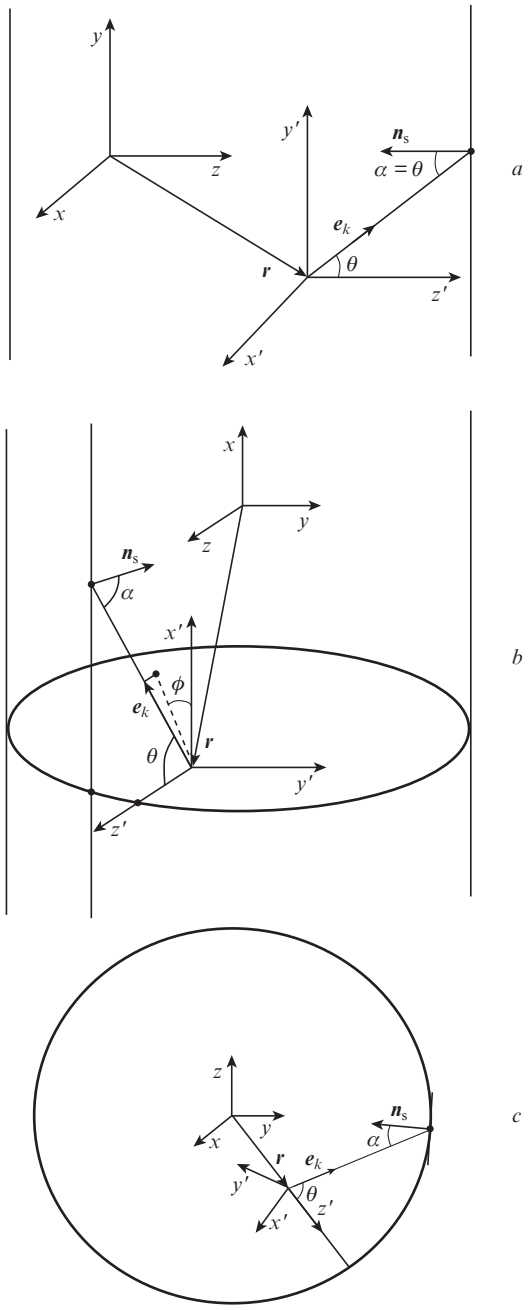

Figure 4. Nanoparticles and auxiliary coordinate systems: (a) flat film, (b) nanowire and (c) nanosphere; $n_{\rm s}$ is the internal normal to the surface of the nanoparticles at point of its intersection with the photoelectron trajectory.

4.3. Nanosphere

Finally, we present expressions corresponding to the case of a spherical nanoparticle (Fig. 4c). The coordinate system $x'y'z'$ is oriented so that the z' axis is perpendicular to the sphere surface, and the other axes are oriented arbitrarily. Integrals (7) and (26) have the form

$$\eta_{\rm i} = 3\int_0^1 \eta_{\rm i}^{\rm local}(\xi)\xi^2\,{\rm d}\xi, \tag{34}$$

$$\eta_{\rm i}^{\rm local}(\xi) = \frac{3}{2}(k_{\hbar\omega}^3 - k_{\rm F}^3)^{-1} \int_0^{\pi}{\rm d}\theta \int_{k_{\rm F}}^{k_{\hbar\omega}} I_{\rm sph}(k,\xi,\theta)\,{\rm d}k, \tag{35}$$

where $\xi = r/R$; r is the distance to the centre of the sphere; R is the radius of the sphere; and the function $I_{\text{sph}}(k,\xi,\theta)$ is written similarly to functions $I_{\text{f}}(k,\xi,\theta)$ and $I_{\text{cyl}}(k,\xi,\theta,\varphi)$, and the dependences of α and L on the integration variables have the form

$$\alpha(\xi,\theta) = \arcsin(\xi\sin\theta),$$
$$L(\xi,\theta) = R[\sqrt{1-(\xi\sin\theta)^2} - \xi\cos\theta]. \tag{36}$$

In the case of the '0–1' model at $r_m = 1$ and $l_{\text{e}} = \infty$, the integral in (34) can be calculated analytically [8]:

$$\eta_{\text{i}} = \frac{1}{\delta^{3/2}-1}\left\{\delta^{3/2} - \gamma^{-3/2}\left[\frac{3}{2}\ln(\gamma\delta)+1\right]\right\}. \tag{37}$$

4.4. Spectral dependence of the IQE

Using the expressions obtained in Sections 4.1–4.3 for η_{i} and $\eta_{\text{i}}^{\text{local}}$, we can construct the spectral dependences of the IQE for various nanoparticles (spherical nanoparticles, cylindrical nanowires) and a flat film (Fig. 5). Numerical calculations are performed for gold nanoparticles surrounded by a GaAs matrix for the following parameters: $r_m = 15$, $\mathcal{E}_{\text{F}} = 5.51$ eV, $W = 6.31$ eV, $l_{\text{e}} = 41$ nm [8, 12]. The calculations were carried out using the '0–1' model. The film thickness and the diameters of the sphere and cylinder were taken equal to 100 nm. One can see from Fig. 5 that the IQE is equal to $\sim 10^{-3}$ at a wavelength of $\lambda = 500$ nm and to $\sim 10^{-6}$ at $\lambda = 1500$ nm and increases monotonically with increasing photon energy. In addition, the calculations show that spherical nanoparticles have the highest IQE (at equal characteristic sizes), the IQE of a cylindrical nanowire and a two-sided film being approximately 1.5 and 3 times smaller, respectively (for a one-sided film the IQE is ~6 times smaller). These relations are carried out with an error of no more than 20%.

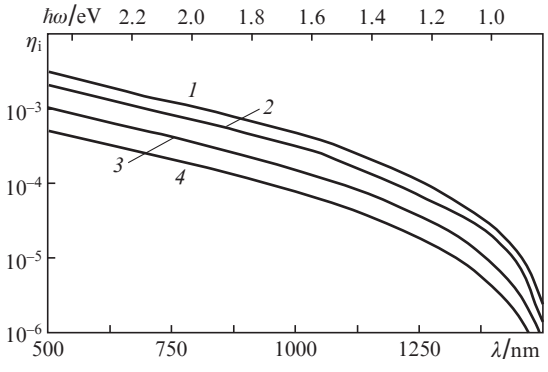

Figure 5. IQE of different nanoparticles as a function of light wavelength λ (or photon energy $\hbar\omega$): (*1*) spherical nanoparticle, (*2*) cylindrical nanowire, (*3*) film with emission of the electrons from both sides and (*4*) film with emission of the electrons from one side.

5. Spectral dependence of the IQE of photoemission from nanoparticles near the long-wavelength boundary

In order to simplify the formulas for the IQE of nanoparticles, use is made of two approximations.

1. The energy of the photoelectron is only slightly greater than the barrier height so that $\hbar\omega \approx W - \mathcal{E}_{\text{F}}$.

2. In calculating the photoelectron exit cone, the boundary is considered flat. This approximation is fulfilled either in a film with flat boundaries or under the condition that the mean free path of an electron, l_{e}, is much smaller than the characteristic size of the nanoparticles: $l_{\text{e}} \ll L_{\text{n}}$. In this case, the photoelectrons can only penetrate the matrix from a thin surface layer of the metal whose thickness is on the order of l_{e}.

With these assumptions being realised, the wave vectors of the photoelectrons overcoming the potential barrier at the interface are located inside the exit cone with a small opening angle and axis directed along the normal to the nanoparticle boundary (in the case of a flat film these are two coaxial cones with a common vertex). In this case, the axis of the polar coordinate system, which is used to calculate integral (26), can be directed for convenience along the normal to the nanoparticle surface and we assume that $\sin\theta \approx \theta$, $\cos\theta \approx 1$, and therefore $L(\boldsymbol{r}) = L_{\text{s}}(\boldsymbol{r})/\cos\theta \approx L_{\text{s}}(\boldsymbol{r})$, where $L_{\text{s}}(\boldsymbol{r})$ is the shortest distance from point of the photoelectron generation to the nanoparticle surface (length of the normal to the surface drawn from the point of the photoelectron generation). From formulas (7) and (26) for the IQE of the nanoparticle we obtain the expressions

$$\eta_{\text{i}} = G_{\text{str}} G_D,$$
$$G_{\text{str}} = \frac{1}{V_{\text{n}}}\int_{V_{\text{n}}} \exp\left[-\frac{L_{\text{s}}(\boldsymbol{r})}{l_{\text{e}}}\right]\mathrm{d}^3 r, \tag{38}$$
$$G_D = \frac{2\pi}{V_k}\int_0^{\theta_{\max}} \theta\,\mathrm{d}\theta \int_{k_{\min}(\theta)}^{k_{\max}} k^2 D(\mathcal{E}(k),\theta)\,\mathrm{d}k,$$

where

$$k_{\min}(\theta) \approx \left(\frac{2mW}{\hbar^2}\right)^{1/2}\left(1+\frac{r_m}{2}\theta^2\right);\ k_{\max} \approx \left(\frac{2mW}{\hbar^2}\right)^{1/2}\left(1+\frac{Z}{2}\right);$$
$$Z = \frac{\hbar\omega - (W-\mathcal{E}_{\text{F}})}{W};\ \theta_{\max} = \left(\frac{Z}{r_m}\right)^{1/2};\ \text{and}$$
$$V_k \approx \frac{4}{3}\pi\left(\frac{2m}{\hbar^2}W\right)^{3/2}\left[1-\left(\frac{\mathcal{E}_{\text{F}}}{W}\right)^{3/2}\right].$$

In formula (38), the parameter G_{str} is a structural factor that depends only on the nanoparticle shape and the mean free path of the photoelectron, and G_D is a factor that depends only on the chosen formula for the transmission coefficient D.

For D of form (21) (a rigorous solution for a rectangular potential step) and for D of form (24) ('0–1' model), we can write the approximate expression for G_D:

$$G_D = \frac{a}{r_m^{\beta}}\left[1-\left(\frac{\mathcal{E}_{\text{F}}}{W}\right)^{3/2}\right]^{-1} Z^{\alpha}, \tag{39}$$

where $a = 5/12$, $\alpha = 5/2$ and $\beta = 0.65$ for D of form (21) and $a = 3/16$, $\alpha = 2$ and $\beta = 1$ for D of form (24). As was noted above, expressions (21) and (24) for the transmission coefficient are limiting and therefore for other potentials (at least those for which the tunnelling effects are insignificant) the exponents in (39) must be in the range of $2 \leqslant \alpha \leqslant 2.5$ and $1 \geqslant \beta \geqslant 0.65$.

One can see from (39) that at not too large photon energies the account for the jump of the effective electron mass at

the metal–semiconductor interface always reduces the IQE of the nanoparticle, and this reduction is described by a simple (exponential) dependence of the IQE on the ratio of effective masses of electrons in the metal and semiconductor. This allows one, without numerical calculations, to estimate immediately a decrease in the IQE due to the effective mass jump. For example, for gold nanoparticles in a GaAs matrix the account for the jump of the effective electron mass provides an IQE reduction by 6–15 times, depending on the chosen model of the transmission coefficient.

The analytical expression for the structural factor $G_{\rm str}$ in the case of a flat film with an arbitrary $l_{\rm e}$ has the form

$$G_{\rm str} = N_{\rm sd}\frac{l_{\rm e}}{L_{\rm f}}\left[1 - \exp\left(-\frac{L_{\rm f}}{l_{\rm e}}\right)\right], \tag{40}$$

and for other structures with curvilinear boundaries at $l_{\rm e} \ll L_{\rm n}$

$$G_{\rm str} = l_{\rm e}\frac{S_{\rm n}}{V_{\rm n}}, \tag{41}$$

where $S_{\rm n}$ is the surface area of the nanoparticle. For a sphere of radius R, the structural factor $G_{\rm str} = 3l_{\rm e}/R$, and for a cylinder of radius R, $G_{\rm str} = 2l_{\rm e}/R$. Then, at equal characteristic sizes of the sphere, cylinder and two-sided film, the ration of their IQEs is 3 : 2 : 1, respectively. The numerical calculations show that the ratio is fulfilled within tens of percent at an arbitrary $l_{\rm e}$ (including $l_{\rm e} = \infty$).

In this paper the IQE was calculated numerically for a 100-nm-thick two-sided gold film surrounded by a GaAs matrix (Fig. 6). Figure 6a presents the results of numerical calculations by the '0–1' model and rectangular potential step model with and without the effective mass of the jump taken into account. The data of Figure 6a allows one to draw two conclusions. Firstly, the '0–1' model gives a higher IQE value as compared to the rectangular potential step model. Secondly, a difference in the results obtained for these models decreases with increasing r_m (dashed curves calculated by taking into account the effective electron mass jump are far less different than the solid curves calculated without this jump taken into account). The first is related to the fact that $D_{\rm q}(\mathcal{E},\theta) \leqslant D_{0-1}(\mathcal{E},\theta)$ for any electron energies $\mathcal{E}$ and angles θ of its incidence on the boundary, and the second to the fact that, according to formula (39), the IQE calculated by the '0–1' model decreases with increasing r_m faster than the IQE calculated using the exact solution for a rectangular potential step ($\propto 1/r_m$ vs. $\propto 1/r_m^{0.65}$). Thus, if the jump of the mass is sufficiently large, it does not matter what model of the potential is used: 'extremely sharp' or 'extremely smooth'; therefore; in calculations use can be made of a simpler '0–1' model with an extremely smooth change in the potential. This conclusion should be further verified in the case when the tunnelling effects on the boundary are significant.

Figure 6b shows the dependences $\eta_{\rm i}(\hbar\omega)$ calculated numerically and analytically by formula (39) taking into account the effective mass jump. One can see that the numerical and analytical results are pretty close, although formula (39) better describes the dependence $\eta_{\rm i}(\hbar\omega)$ calculated by the '0–1' model for the transmission coefficient than that calculated by the rectangular potential step model. This is due to the absence of the approximation error of the transmission coefficient in the derivation of relation (39) for the '0–1' model.

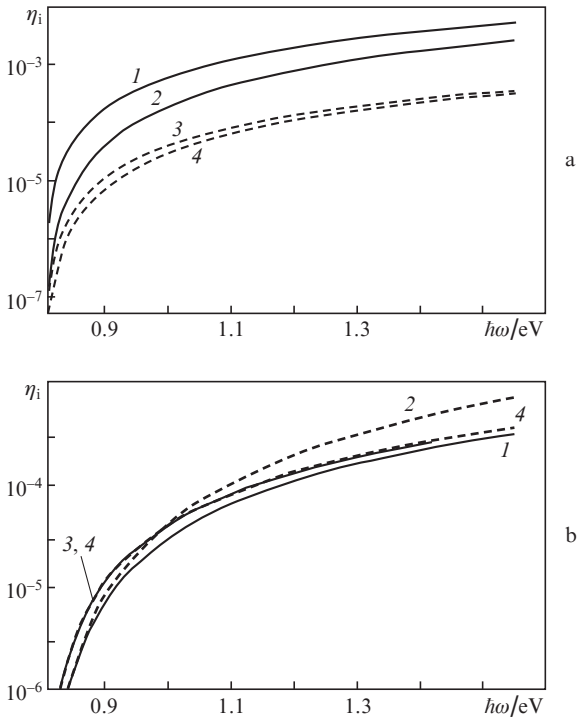

Figure 6. IQE of a two-sided gold film in a GaAs matrix as a function of photon energy: (a) numerical calculation using (*1*, *3*) '0–1' model and (*2*, *4*) rectangular potential step model for the transmission coefficient D without (*1*, *2*) and with (*3*, *4*) the effective electron mass jump taken into account, and (b) (*1*, *3*) numerical calculation and (*2*, *4*) calculation of formula (39) using a rigorous solution for (*1*, *2*) a rectangular potential step and (*3*, *4*) '0–1' model with the effective electron mass jump taken into account.

6. Conclusions

In this paper we have obtained expressions for the IQE of the bulk photoelectric effect for metal nanoparticles and flat films in a semiconductor matrix. The consideration takes into account the jump of the effective electron mass at the nanoparticle–matrix interface and the cooling effect of hot electrons due to electron–electron collisions. Using the example of photoemission from gold nanoparticles into a GaAs matrix we have shown that the account for the effective electron mass jump reduces the IQE by 6–15 times depending on the chosen model of the transmission coefficient of the Schottky barrier.

Expressions are obtained for the spectral dependence of the IQE in the approximation of a plane boundary for a flat film and nanoparticles of two types (nanosphere and nanowire with a circular cross bsection) and for two models of the transmission coefficient at the nanoparticle–matrix interface: exact quantum-mechanical solution for a rectangular potential step (rectangular potential step model) and its approximation by the Heaviside function ('0–1' model). For a sphere, cylinder and two-sided flat film with the same characteristic dimensions the found IQE ration equals 3 : 2 : 1. This ratio is fulfilled accurately, provided that the mean free path $l_{\rm e}$ of the photoelectron in the scattering is much smaller than the characteristic size of the nanoparticle, and with an accuracy of 20% at an arbitrary $l_{\rm e}$ (including $l_{\rm e} = \infty$). Thus, the nanostructuring of metals not only leads to increased local fields due to plasmon excitation, but also increases the probability that

electrons will reach the boundary of the nanoparticle with the matrix before it loses energy in other collisions.

The impact of the effective mass jump of the photoelectron during its passage through the boundary manifests itself not only in the reduction of the IQE. It turns out that if r_m (the ratio of the effective masses of the electron in the metal and semiconductor) is 10 or higher (such as in the case of photoemission from gold into GaAs), the results of IQE calculations are weakly dependent on the model of the potential at the boundary, at least if the tunnelling effects are not taken into account. We have proposed analytical formulas for calculating the IQE to ensure that the results are in good agreement with numerical calculations.

In the calculations we have taken into account not all the effects of the impact of the actual shape of the potential barrier on the passage of electrons across the interface; in particular, we have not considered the tunnelling of electrons. In the future, these effects can be taken into account in the numerical calculations by introducing the appropriate expression for the IQE of the dependence of the transmission coefficient on the electron energy for the barriers of a more realistic shape [27].

For nanoparticles of more complex (than those discussed in this paper) shape, one should take into account the nonuniform field distribution inside the particle. This inhomogeneity can be accounted for by the spatial dependence of the factor $\hat{F}$ [see expression (1)], which is of no importance for numerical calculations of the IQE.

The results can be used to design promising highly sensitive photodetectors and photovoltaic devices. In particular, it is expected that hot electron photoemission will find applications to increase the operating spectral range of solar cells and thus their efficiency. In addition, the effects studied will be used in the development of photoconductive metamaterials.

Acknowledgements. This work was financially supported by the Russian Foundation for Basic Research (Grant Nos 13-08-01438 and 15-02-03152).

References

1. Knight M.W., Sobhani H., Nordlander P., Halas N.J. *Science*, **332**, 702 (2011).
2. Protsenko I.E., Uskov A.V. *Usp. Fiz. Nauk*, **182** (5), 543 (2012).
3. Scales Ch., Berini P. *IEEE J. Quantum Electron*., **46** (5), 633 (2010).
4. Novitsky A., Uskov A.V., Gritti C., Protsenko I.E., Kardynal B.E., Lavrinenko A.V. *Prog. Photovoltaics Res. Appl*., **22** (4), 422 (2014).
5. Leenheer A.J., Narang P., Lewis N.S., Atwater H.A. *J. Appl. Phys*., **115**, 134301 (2014).
6. Stuart R., Wooten F., Spicer W.E. *Phys. Rev*., **135**, A495 (1964).
7. Chen Q.Y., Bates C.W. *Phys. Rev. Lett*., **57** (21), 2737 (1986).
8. Uskov A.V., Protsenko I.E., Ikhsanov R.Sh., et al. *Nanoscale*, **6**, 4716 (2014).
9. Govorov A.O., Zhang H., Gun'ko Y.K. *J. Phys. Chem. C*, **117**, 16616 (2013).
10. Koropov A.V. *Fiz. Tverd. Tela*, **46** (8), 1460 (2004).
11. Davydov S.Yu., Lebedev A.A., Tikhonov S.K. *Fiz. Tekh. Poluprovodn*., **31** (5), 597 (1997).
12. Sze S.M. *Physics of Semiconductor Devices* (New York: Wiley, 1981; Moscow: Mir, 1984).
13. Chen I.-S., Jackson T.N., Wronski C.R. *J. Appl. Phys*., **79**, 8470 (1996).
14. Myrtveit T. *Appl. Surf. Sci*., **73**, 225 (1993).
15. Maier S.A. *Plasmonics: Fundamentals and Applications* (New York: Springer, 2007).
16. Smith N.V. *CRC Crit. Rev. Solid State Sci*., **2** (1), 45 (1971).
17. Berglund C.N., Spicer W.E. *Phys. Rev*., **136**, A1030 (1964).
18. Fowler R.H. *Phys. Rev*., **38**, 45 (1931).
19. Kadlec J., Gundlach K.H. *Phys. Status Solidi A*, **37**, 11 (1976).
20. Ivanov V.G., Panasenkov V.I., Ivanov G.V. *Fiz. Tekh. Poluprovodn*., **31** (6), 735 (1997).
21. Dalal V.L. *J. Appl. Phys*., **42** (6), 4274 (1971).
22. Schmidt M., Brauer M., Hoffmann V. *J. Phys. D: Appl. Phys*., **30**, 1442 (1997).
23. Andreev A.F. *Usp. Fiz. Nauk*, **105** (1), 113 (1971).
24. Brodsky A.M., Gurevich Yu.Ya. *Teoriya elektronnoi emissii iz metallov* (Theory of Electron Emission from Metals) (Moscow: Nauka, 1973).
25. Bastard G. *Phys. Rev. B*, **24** (10), 5693 (1981).
26. Galitsky V.M., Karnakov B.M., Kogan V.I. *Zadachi po kvantovoi mekhanike* (Problems in Quantum Mechanics) (Moscow: Nauka, 1992).
27. Vostokov N.V., Shashkin V.I. *Zh. Eksp. Teor. Fiz*., **126** (1), 239 (2004).